

## **Supporting Information**

### **Mapping 2D- and 3D-distributions of metal/metal oxide nanoparticles within cleared human *ex vivo* skin tissues**

George J. Touloumes,<sup>1,1</sup> Herdeline Ann M. Ardoña,<sup>1,1</sup> Evan K. Casalino,<sup>1</sup> John F. Zimmerman,<sup>1</sup> Christophe O. Chantre,<sup>1</sup> Dimitrios Bitounis,<sup>2</sup> Philip Demokritou<sup>2</sup> and Kevin Kit Parker<sup>\*,1</sup>

1. Disease Biophysics Group, Wyss Institute for Biologically Inspired Engineering, John A. Paulson School of Engineering and Applied Sciences, Harvard University, Cambridge, MA 02138 USA
2. Center for Nanotechnology and Nanotoxicology, Department of Environmental Health, T. H. Chan School of Public Health, Harvard University, Boston, MA 02115 USA

<sup>1</sup>G. J. T and H. A. M. A. contributed equally.

#### **\*Corresponding author:**

Kevin Kit Parker  
29 Oxford St. (Rm. 321)  
Cambridge, MA, 02138  
Tel: (617) 495-2850  
Fax: (617) 495-9837  
Email: [kkparker@seas.harvard.edu](mailto:kkparker@seas.harvard.edu)

### **Supplementary Methods: *Image analysis/ quantification of nanoparticle distribution***

*Quantification of darkfield scattering intensity:* Uncleared and cleared 50  $\mu\text{m}$  thick skin sections were imaged in darkfield mode under identical acquisition settings using an integrated darkfield hyperspectral and Raman microscope. Images were acquired via LabSpec 6.4.4 software, with lamp intensity kept the same for all samples. For each image, the epidermis and dermis were manually traced using ImageJ and the mean pixel intensity of each region was recorded. The results (Fig. 2f) were pooled from at least 8 images from different sections of the same tissue sample.

*Calculation of % pixel coverage from hyperspectral images:* All map images from ENVI were post-processed in ImageJ and converted to an 8-bit type binary image. An area of  $250 \times 300$  pixels was selected prior to running the particle analysis plug-in to measure the area fraction of the pixels in the hyperspectral map. For each exposure condition, images from tissue sections of three different sample tissues with 3 fields of view (FOV) per section were recorded; yielding a total of at least 9 FOV per condition that were post-processed for % pixel coverage measurements.

*Quantification of Ag nanoparticle coverage area in wounded skin tissues:* The images used for quantifying nanoparticle coverage in skin biopsies with wounded epidermis were obtained using light-sheet fluorescence microscopy (LSFM). Each full-thickness ( $\sim 5$  mm) skin biopsy was imaged as a Z-series and reconstructed using Imaris Bitplane software. After taking snapshots of the Imaris 3D renderings such that the full epidermis was in plain view and orthogonal to the camera axis, ImageJ was used for pixel quantification. We started by binarizing the AgNP channel by selecting an intensity threshold such that only the nanoparticles were included and any background signal was eliminated from the area calculation. In the wounded samples, the borders

of the wound were marked and the area of the nanoparticles within the wound was divided by the wound's total area to produce a measurement of the percent coverage of AgNPs within the wound.

*Approximation of Ag nanoparticle permeation depth in wounded skin tissues:* Images of wounded skin tissues exposed to Ag-647 ENMs were obtained using LSM and processed using ImageJ. Each image was a 15  $\mu\text{m}$ -thick optical section of the intact 5 mm full thickness tissue. In ImageJ, Ag-647 ENMs at the outermost surface of the tissue were randomly selected and paired with the corresponding Ag-647 ENM which had permeated deepest into the tissue at the same X coordinate. The Y coordinate difference between the outermost and innermost ENMs at the same X coordinate was taken to be the permeation depth into the tissue.

*Statistical analysis:* Comparison between test groups was carried out using a two-tailed Student's *t*-test. All data were presented as mean  $\pm$  SEM, unless otherwise specified. For each data set, the corresponding annotations for *p* values can be found in each figure caption.

**Supplementary Table 1.** Protocol variations for immunostaining and iDISCO+ clearing of human skin tissue samples studied herein.

Step	Uncleared Tissue Sections	Cleared Tissue Sections for Confocal, Darkfield, or Hyperspectral Imaging	Cleared Tissue Sections for Raman spectroscopy	Uncleared Whole Tissue Samples	Cleared Whole Tissue Samples
OCT embedding	yes	yes	yes	no	no
Cryostat sectioning	yes	yes	yes	no	no
OCT removal in H <sub>2</sub> O	3x 5 mins	3x 5 mins	3x 5 mins	no	no
Pretreatment - 20% methanol increment dehydration	no	no	no	1 h each	1 h each
Pretreatment - delipidation in 66% DCM - 33% MeOH	no	no	no	3 h	3 h
Pretreatment - wash in methanol	no	no	no	2 × 1 h	2 × 1 h
Pretreatment - bleach in 5% H <sub>2</sub> O <sub>2</sub> in MeOH	no	no	no	overnight at 4°C	overnight at 4°C
Pretreatment - rehydrate in MeOH and wash in PTx.2	no	no	no	1 h each	1 h each
Immunostaining - permeabilization	30 min at 37°C	30 min at 37°C	30 min at 37°C	overnight at 37°C	overnight at 37°C
Immunostaining - blocking	1 h at 37°C	1 h at 37°C	1 h at 37°C	overnight at 37°C	overnight at 37°C
Immunostaining - primary antibodies	overnight at 4°C	overnight at 4°C	overnight at 4°C	48 h at 37°C	48 h at 37°C
Immunostaining - PTwH wash	3 × 5 min	3 × 5 min	3 × 5 min	overnight	overnight
Immunostaining - secondary antibodies	2 h	2 h	2 h	48 h at 37°C	48 h at 37°C
Immunostaining - PTwH wash	3 × 5 mins	3 × 5 mins	3 × 5 min	overnight	overnight
Immunostaining - mounting in PBS	yes	no	no	yes	no
Clearing - 20% methanol increment dehydration	no	5 min each	5 min each	no	1 h each
Clearing - delipidation in 66% DCM - 33% MeOH	no	1 h	1 h	no	at least 3 h, until samples sink

**Supplementary Table 2.** Complete tabulated results from ICP-MS analysis (Ti and Zn content) of solvent blanks; report units =  $\mu\text{g}/10\text{ mL}$ .

Sample	$^{47}\text{Ti}$ (MR); $\pm$		$^{49}\text{Ti}$ (MR); $\pm$		$^{66}\text{Zn}$ (MR); $\pm$		$^{68}\text{Zn}$ (MR); $\pm$	
PBS blank, Trial 1	0.003	0.004	0.003	0.003	0.009	0.010	0.022	0.012
MeOH blank, Trial 1	0.002	0.005	0.001	0.002	0.056	0.016	0.054	0.011
DBE blank, Trial 1	0.018	0.013	0.016	0.015	0.033	0.009	0.041	0.019
PBS blank, Trial 2	0.001	0.001	0.001	0.001	0.012	0.001	0.012	0.001
MeOH blank, Trial 2	0.001	0.006	0.000	0.001	0.125	0.004	0.118	0.005
DBE blank, Trial 2	0.000	0.001	0.000	0.001	0.015	0.001	0.014	0.002

Notes: (a) MR = medium resolution; (b)  $\pm$  are the propagated uncertainty values from the triplicate analysis and sample subtraction).

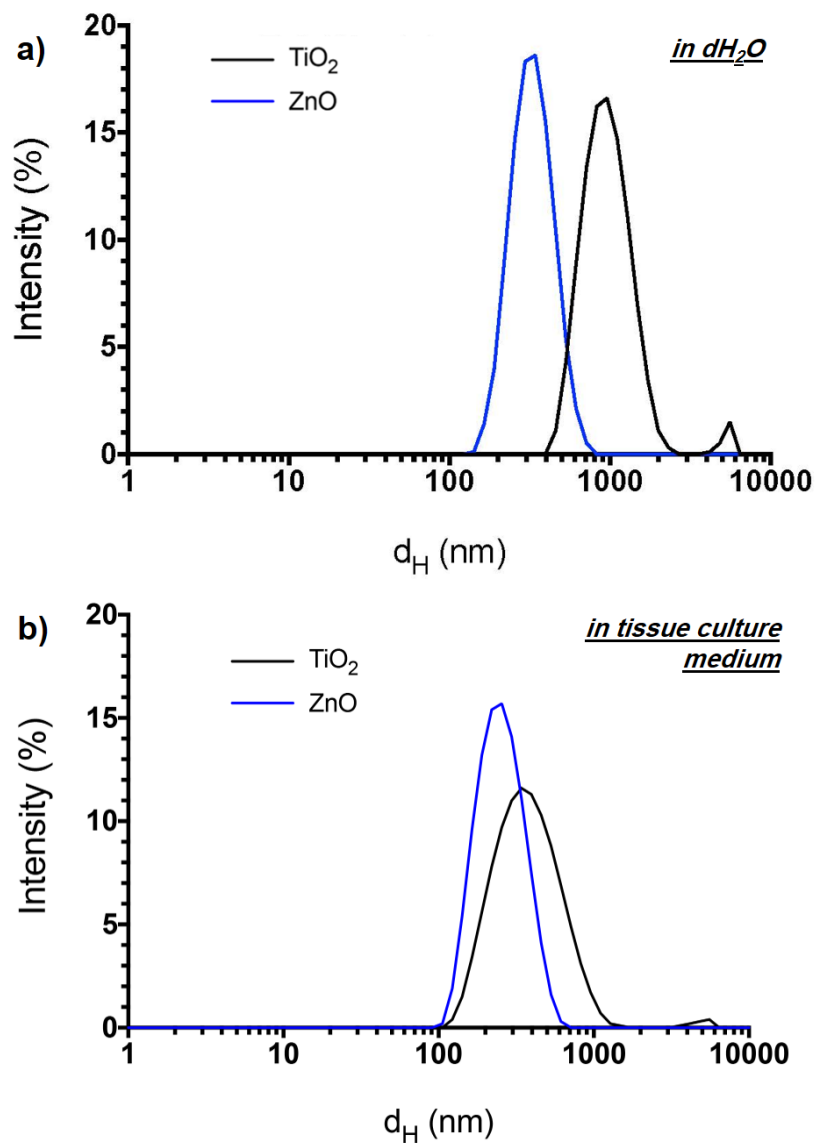


**Figure S1. Intensity-weighted hydrodynamic size ( $d_H$ ) distributions of the ENMs used in this study as measured by dynamic light scattering (DLS).** (a) Dispersion in deionized water at 500  $\mu\text{g/mL}$  by cup-horn sonication based on their respective  $\text{DSE}_{\text{cr}}$  values. (b) Dispersion in tissue culture medium at 100  $\mu\text{g/mL}$ . TiO<sub>2</sub> (—); ZnO (—).

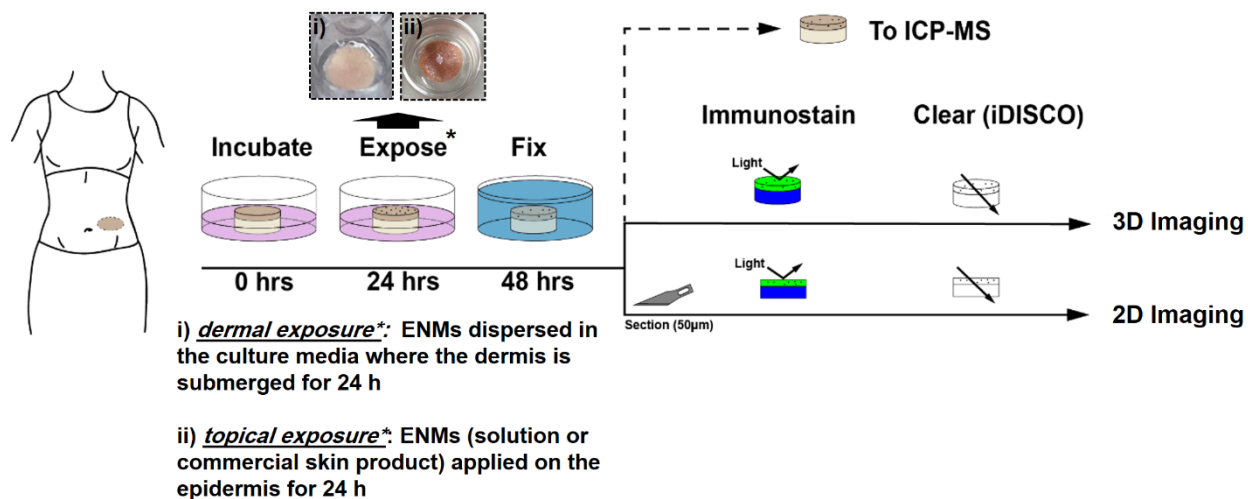


**Figure S2. Schematic illustration of experimental workflow for this study.** Commercially available skin biopsies from collected from patients’ abdominal regions were incubated at 37°C and 5% CO<sub>2</sub> while maintaining an air-liquid interface in which the epidermal side was exposed to air. The dermal side was submerged in the tissue culture medium provided by the vendor (Genoskin). For both epidermally and dermally ENM-exposed tissues, ENMs were added as a suspension in the tissue culture medium where the samples were submerged. After 24 h of exposure, samples were fixed with 4% paraformaldehyde at 4°C for 24 h before proceeding to tissue processing and analysis. Exposed and fixed samples were then stored and shipped for ICP-MS analysis, or immunostained, cleared whole, and imaged in 3D with a light sheet microscope, or sectioned at 50 µm thickness. 50 µm thick skin slices were subsequently immunostained, cleared, and analyzed by a combination of confocal and darkfield microscopy and Raman and hyperspectral spectroscopy. *Inset*: Photograph of representative skin biopsies, with the dermal portion submerged in culture media and the epidermis exposed to air; i) healthy skin biopsies used in dermal exposure and ii) skin biopsies with 2 mm epidermal wounds used in topical exposure experiments.

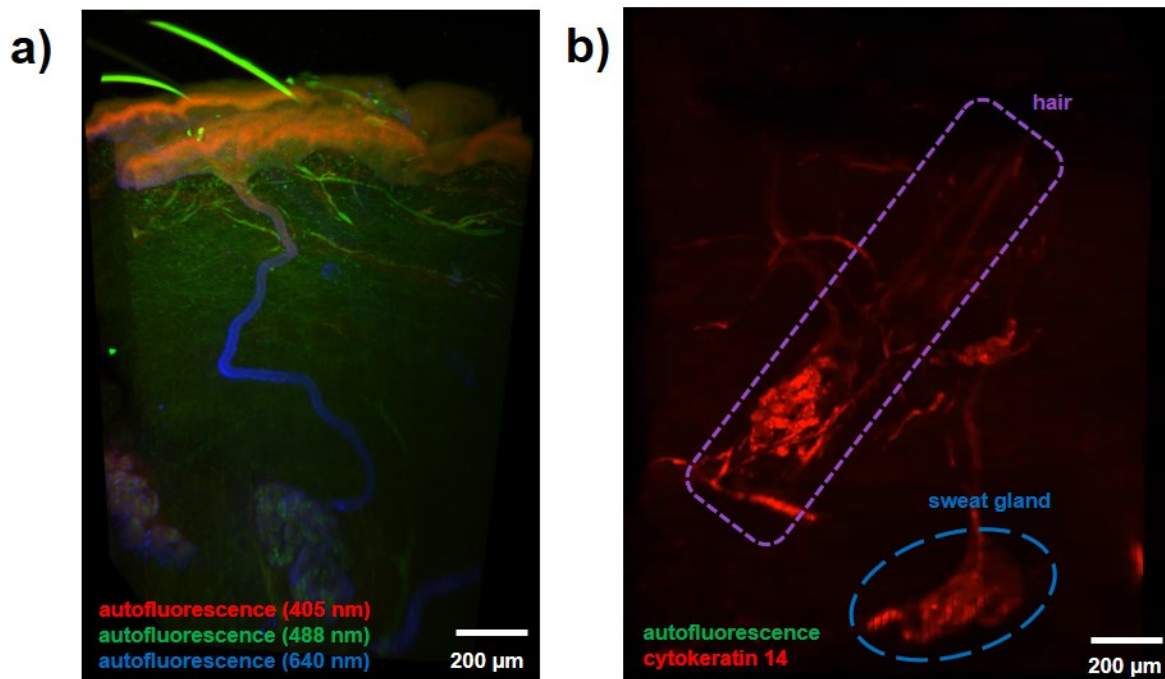


**Figure S3. Identifying skin appendages based on detectable autofluorescence and immunofluorescence signals in full-thickness skin tissues using light sheet microscopy.** (a) Imaris 3D reconstruction of a skin tissue region with visible hair follicles and glands, rendered the maximum intensity project of a Z stack. (b) 3D reconstruction of a skin region immunolabeled for cytokeratin 14 and highlighting identifiable appendages. Full 360° view of the 3D rendering for Fig. S2b is available in Video S1.



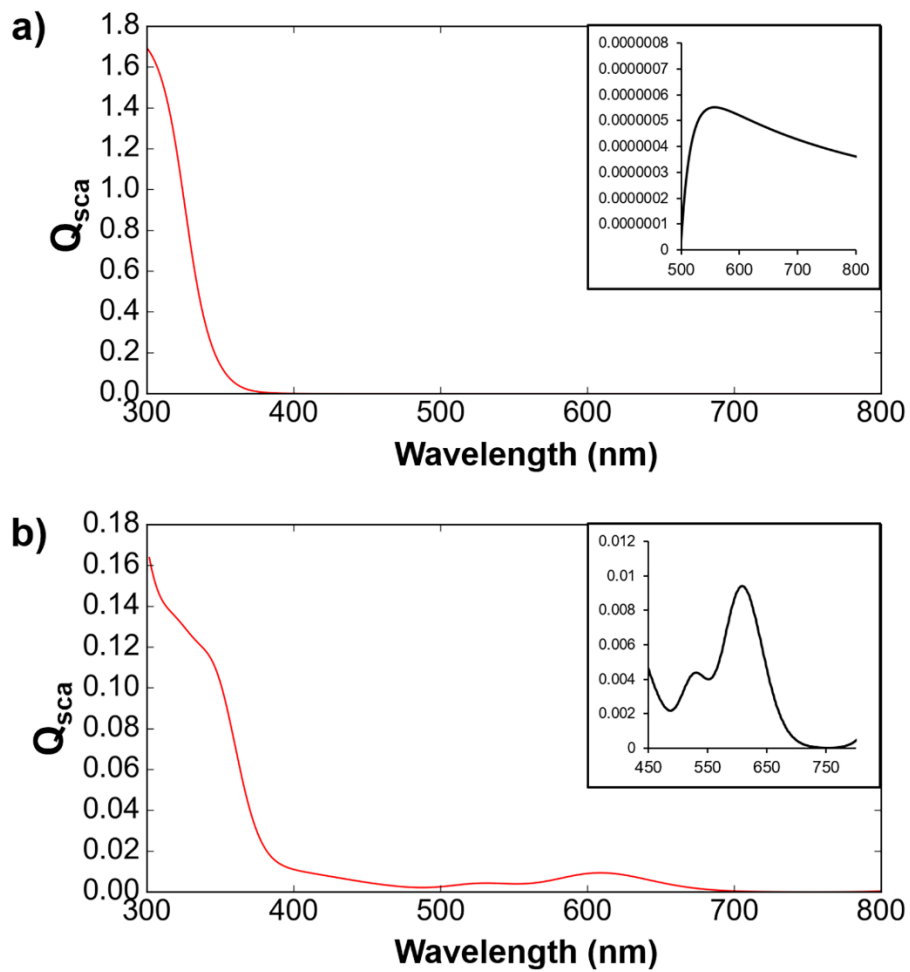


**Figure S4. Predicted scattering profiles ( $Q_{sca}$ ) of individual nanoparticles in this study. (a)  $\text{TiO}_2$  (100 nm) and (b)  $\text{ZnO}$  (50 nm), using Lorenz-Mie theory calculations. *Inset*: zoomed in spectra in the 500-800 nm and 450-800 nm window for  $\text{TiO}_2$  and  $\text{ZnO}$ , respectively.**

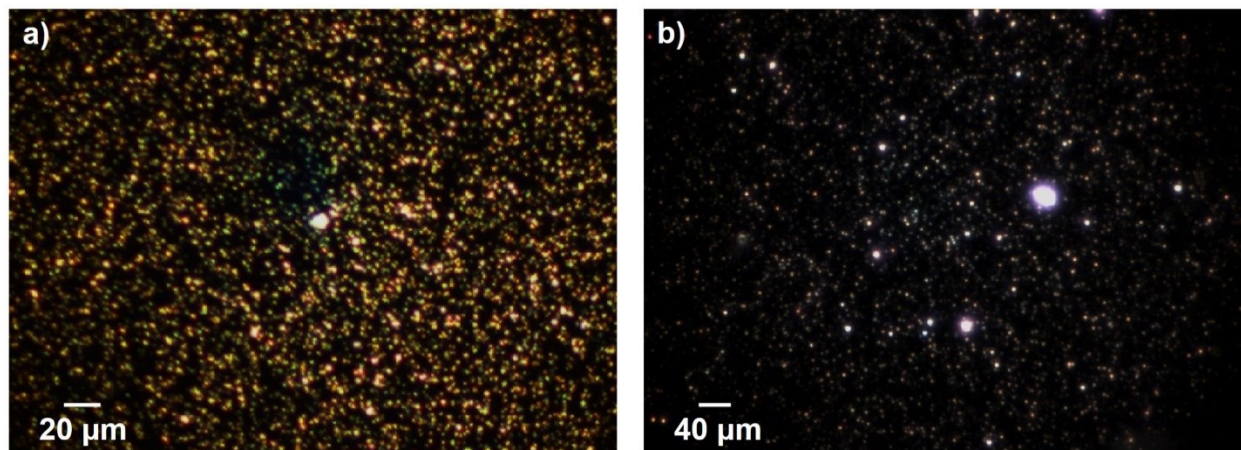


**Figure S5. Representative darkfield images of reference aqueous solutions of ENMs.** (a)  $\text{TiO}_2$  and (b)  $\text{ZnO}$  nanoparticles. Solutions were prepared at  $100 \mu\text{g/mL}$ , then were mounted on a glass slide for imaging. Both images were acquired under the same lamp intensity and exposure conditions.

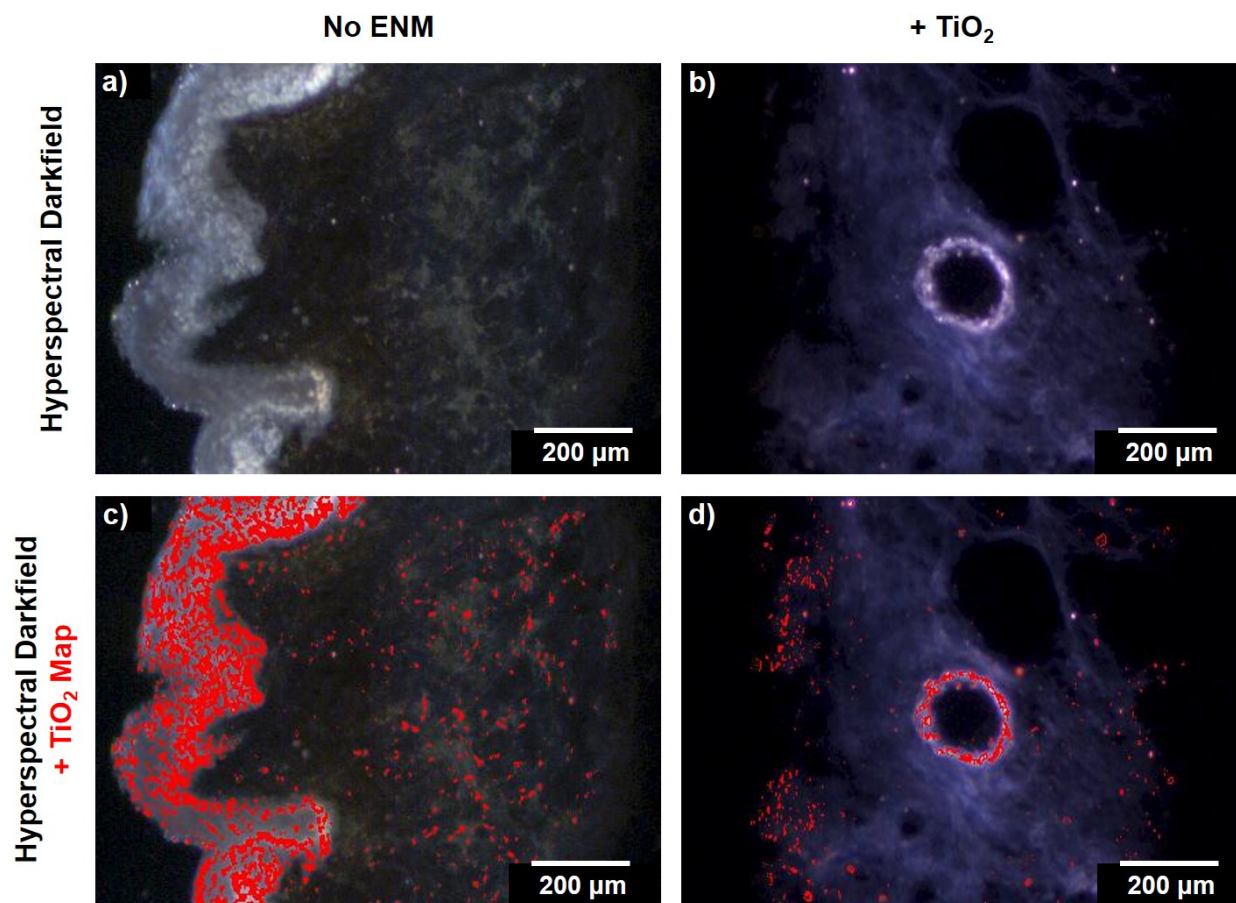


**Figure S6. Human skin tissues dermally exposed to 100 μg/mL TiO<sub>2</sub> suspension for 24 h.** Hyperspectral darkfield images (a, b) with TiO<sub>2</sub>-positive pixel map (c, d; annotated in red). Taken from tissue sections without treatment (a, c) and from the TiO<sub>2</sub>-treated tissues (b, d).